

ATTITUDE ESTIMATION FOR PICOSATELLITES WITH DISTRIBUTED COMPUTING PLATFORM USING MURRELL'S ALGORITHM OF THE EXTENDED KALMAN FILTER

Sharan Asundi*, Haniph Latchman[†] and Norman Fitz-Coy[‡]

Picosatellites have limited capabilities for hosting precise attitude and inertial sensors and the available computational resources are at premium. SwampSat is one such picosatellite under development at the University of Florida with the objective of demonstrating precision three axes attitude control. The satellite hosts a distributed computing system comprised of a low power flight computer and a high speed digital signal processor (DSP). The flight computer, designed to execute routine operations, is interfaced with coarse attitude sensors. The DSP, operated intermittently, interfaces with an inertial measurement unit and hosts Murrell's version of the extended Kalman filter, designed for computationally limited satellites. The work presented describes the attitude estimation algorithm adapted for the distributed computing platform of SwampSat and the mission design for enabling it on orbit during attitude determination and control maneuvers. Results of the simulations carried out to evaluate the need for an estimation algorithm for SwampSat and its effectiveness are discussed.

INTRODUCTION

For smallsats in low Earth orbits, precision three axes attitude control with high slew rates or rapid retargeting and precision pointing (R2P2)¹ is a desired capability.² SwampSat is a picosatellite under development at the University of Florida with the mission objective of demonstrating R2P2 capability for pico- and nanosatellites with an experimental control moment gyroscopes (CMG) based attitude control system (ACS).^{3,4} SwampSat mission specifically addresses key operational objectives and challenges for pico- and nanosatellites, including those specified by the National Aeronautics and Space Administrations (NASA) Franklin and Edison programs.²

Effective and efficient attitude estimation is a critical prerequisite for demonstrating precision three-axis attitude control for SwampSat and it is the driving motivation for the work presented. The paper describes an attitude estimation algorithm adapted for a picosatellite with a distributed computing platform hosting coarse Sun sensors, a micro electro mechanical system (MEMS) magnetometer and a MEMS inertial measurement unit (IMU). It discusses the need for an effective and efficient estimation algorithm, its adaptation on a distributed computing platform, the design for on-orbit operation and the results of the simulations evaluating its effectiveness. The estimation algorithm is designed by coupling QUaternion ESTimator (QUEST)⁵ with Murrell's version⁶ of the extended Kalman filter (EKF)⁷⁻⁹ as described in Reference 10. The two algorithms are coupled for faster convergence of the attitude estimate with the true attitude.

*Graduate Student, Mechanical and Aerospace Engineering, University of Florida, Gainesville, FL 32611.

[†]Professor, Electrical and Computer Engineering, University of Florida, Gainesville, FL 32611.

[‡]Associate Professor, Mechanical and Aerospace Engineering, University of Florida, Gainesville, FL 32611.

SWAMPSAT ARCHITECTURE AND COMPUTING PLATFORM

SwampSat is designed around the CubeSat specification¹¹ and form factor. The architecture of SwampSat is primarily subsystem based and each subsystem's hardware is designed around separate electronic boards. SwampSat uses commercial-off-the-shelf (COTS) components for the electrical power system (EPS) and the communication subsystems. The ACS, attitude determination system (ADS), command and data handling (CDH) system and the structure are designed in house. The subsystems are all designed or selected to address the size weight and power (SWaP) constraints of the CubeSat specification and the SWaP requirements of SwampSat. The structural and thermal subsystem is designed to withstand the space environment and the satellite chassis is dimensionally designed to fit in a Poly Picosatellite Orbital Deployer (P-POD).¹² The layout shown in Figure 1 explains the architecture of SwampSat and the interface connections between subsystems.

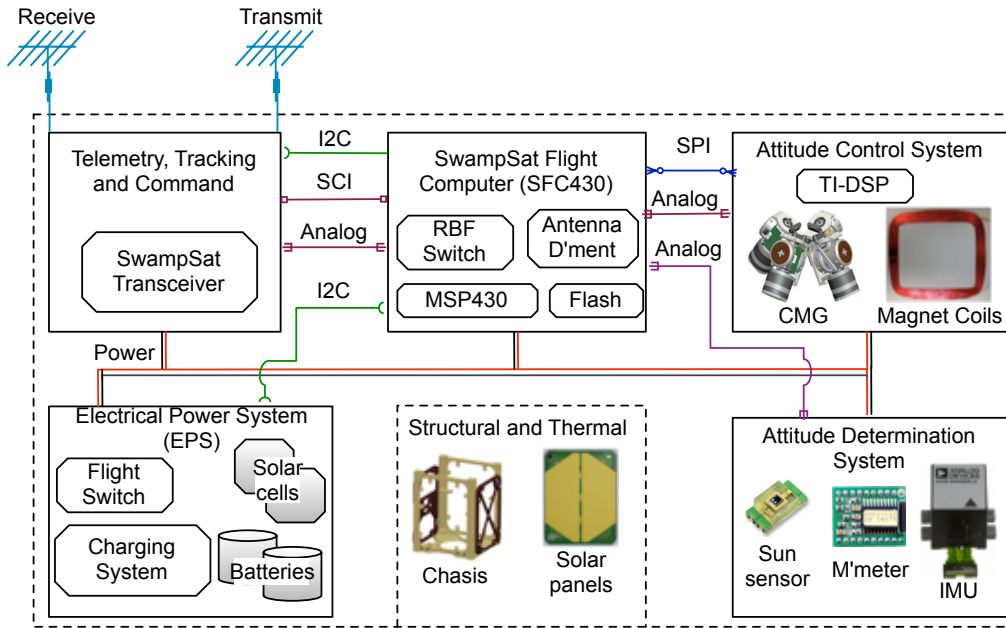


Figure 1. SwampSat Architecture

The on orbit power generating capability (1.5 W) of SwampSat limits the continuous operation of its high performance processor selected for precision computing.¹³ The flight computer, although suited well for routine operations is limited in its ability to support the computational requirements of the attitude determination and control system. To address these limitations SwampSat computing platform is designed as a distributed system. An MSP430¹⁴ based flight computer, identified as SFC430, is in continuous operation and the CMG controller, a high performance digital signal processor (DSP)¹⁵ from Texas Instruments (TI), is operated intermittently to perform attitude operations.

Distributed Operation

SwampSat on orbit is designed to be operated in 5 modes to accommodate its distributed architecture - (i) Safe-hold (ii) Detumble (iii) ADS validation (iv) CMG operations (ACS validation) and (v) Comms. Safe-hold operating mode is designed to validate secondary objectives and consume optimum power during its operation. The detumble operating mode of SwampSat stabilizes the

satellite and evaluates the performance of the electrical power system, particularly the solar cells. The ADS and ACS validation modes are designed to validate the attitude determination and control systems of SwampSat. Mission validating data is stored in flash memory on board during the execution of detumble, ADS and CMG operations. The comms operating mode is designed as a sub routine of the main program to downlink the data to ground control. The safe-hold, detumble and comms operations are executed primarily by the flight computer. SwampSat ADS and ACS validation, designed as distributed operations, are initiated by the flight computer and the mathematics are executed by the DSP. The schematic shown in Figure 2 identifies the main hardware and software components of the distributed attitude determination and estimation system of SwampSat.

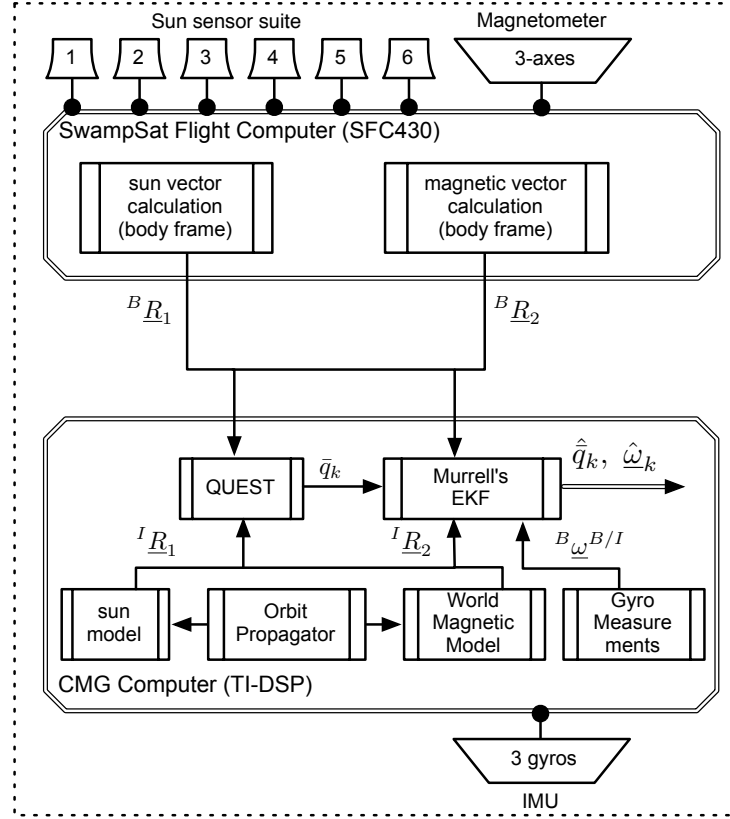


Figure 2. SwampSat ADS as a Distributed System

Attitude determination and estimation algorithms for SwampSat are hosted on the CMG controller. A serial peripheral interface (SPI) link enables communication between SFC430 and the CMG controller. A flowchart demonstrating implementation of the attitude determination and estimation system of SwampSat is shown in Figure 3. Attitude determination is accomplished using QUEST and Murrell's version of the EKF is used for attitude estimation. ADS validation process starts with the execution of the EKF algorithm, which is hosted on the CMG controller and is designed to request attitude vector measurements (body frame) from SFC430 through the SPI link. The reference vectors are requested from the mathematical models, which are implemented on the CMG controller. QUEST is programmed as a sub routine and is invoked from within the EKF with two set of vector measurements as function parameters. The ADS operating mode communicates body vector measurements to the CMG controller on a request basis.

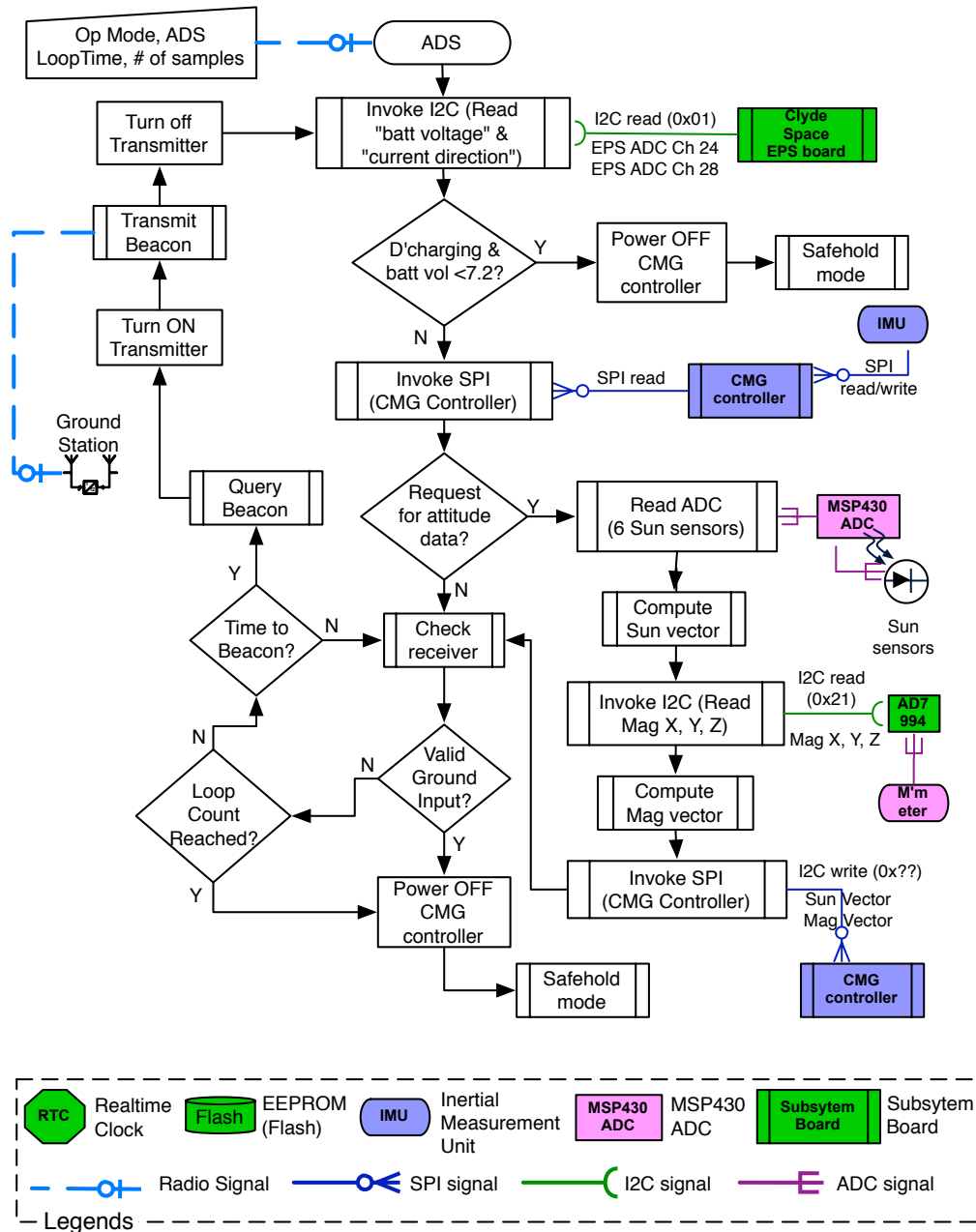


Figure 3. ADS Operating Mode

SWAMPSAT ATTITUDE DETERMINATION AND ESTIMATION

The SwampSat form factor limits the use of a conventional star tracker hence the satellite is designed to accommodate coarse attitude sensors. Primarily, modified light-to-voltage (LTV) converters as sun sensors and a MEMS based magnetometer are interfaced to the SFC430. Additionally, a MEMS based IMU is interfaced to the CMG controller. Initial attitude of the spacecraft is computed as a quaternion using attitude sensors and propagated using IMU.

Attitude Sensors

Although LTVs as coarse sun sensors and MEMS based magnetometers are limited in their ability to precisely determine the reference vectors in the satellite body frame, they are conveniently available in sizes suitable for picosatellite applications and their impact on the satellite power budget is significantly low. If the error sources of these sensors can be mathematically modeled and incorporated they can be effectively used for attitude computations. For SwampSat, LTV based sun sensors are designed and analyzed in house¹⁶ and a sensor model is considered for evaluating the attitude estimation design. A MEMS based magnetometer, the HMC2003 from Honeywell,¹⁷ is selected as the other attitude sensor due to its availability in a form factor suitable for picosatellites and its effectiveness in a low earth orbit (LEO). The maximum magnetic field strength experienced on the earth's surface is limited to 0.6 gauss, as calculated by the International Geophysical Data Center and the HMC2003 is capable of measuring up to ± 2 gauss. The mathematical model considered for these attitude sensors is discussed below.

Attitude sensor model. Let ${}^B \underline{R}_i$ represent the i^{th} measurement of a vector and ${}^I \underline{R}_i$ its representation in a inertial reference frame. The discrete time measurement of the vector and its representation in a reference frame can be modeled to follow Eq. (1).¹⁸

$${}^B \underline{R}_i = \underline{C}_{BI} {}^I \underline{R}_i + \underline{\vartheta}_i \quad (1)$$

Here the sensor error vector $\underline{\vartheta}_i$ is normally distributed random vector with the following properties.

$$\begin{aligned} E\{\underline{\vartheta}_i\} &= \underline{0} \\ E\{\underline{\vartheta}_i \underline{\vartheta}_i^T\} &= \sigma_i^2 \underline{I} \end{aligned}$$

Inertial Sensor

The ADIS16405,¹⁹ a MEMS based IMU from Analog Devices, is identified for measuring the body rates of the satellite. The IMU is equipped with gyros operating in rate mode and can be sampled at frequencies of up to 350 Hz. The ADIS16405 is selected based on a trade study done of the available MEMS based inertial sensors.¹ The low power constraint, port available to interface with the on board computer, operating temperature range and the size/mass were some of the characteristics evaluated for the selection process. The IMU was subjected to analysis and testing to determine the noise and bias characteristics. To verify the integrity of the gyros the IMU was subjected to testing on a rotary table with precision encoders. As discussed in the gyro model below, sensor measurements are affected by drift rate bias and drift rate noise. To determine the distribution of these two components the IMU was placed on a stationary platform and the gyro readings were noted down. The drift rate noise and the drift rate bias were comparable to the output noise and the angular random walk values specified in the sensor data sheet.¹⁹ For evaluating the attitude estimation design, a mathematical model of the gyros, discussed below, is considered.

Gyro model. The gyro model considered was developed by Farrenkopf²⁰ and applied by Hoffman and McElroy.²¹ The gyro model relating the gyro output vector $\underline{\tilde{\omega}}$, the satellite angular velocity $\underline{\omega}$, drift rate bias $\underline{\beta}$ and drift rate noise $\underline{\eta}_1$ is expressed in Eq. (2) and Eq. (3).

$$\underline{\tilde{\omega}} = \underline{\omega} + \underline{\beta} + \underline{\eta}_1 \quad (2)$$

$$\dot{\underline{\beta}} = \underline{\eta}_2 \quad (3)$$

Here η_1 and η_2 are uncorrelated zero-mean Gaussian white-noise processes having the same properties as the sensor error vector $\underline{\vartheta}_i$.

Attitude Estimation

The attitude estimation algorithm adapted for SwampSat is shown in Figure 4. The filter is designed as a 6-state EKF to be implemented in two phases - (i) attitude determination (ii) attitude propagation. The states, which include 3 attitude errors and 3 gyro drift rate biases, are propagated as a 6x6 error covariance matrix. The 3 component attitude error incorporates the inaccuracies in the attitude sensors and the gyro drift rate bias makes up for the inaccuracies in the MEMS gyros.

During the attitude determination phase, the error covariance matrix, P_k^- , is initialized with values determined from experiments, models and component data sheets of the attitude sensors and gyros. The initial bias of the gyros, $\hat{\beta}_k^-$, is assigned to be zero. The sun and magnetic field vector are acquired in the body and inertial frames to initialize the CubeSat attitude quaternion, \hat{q}_k^- , from QUEST. The corresponding attitude matrix, \underline{C}_{BI} and the vector part of the quaternion is computed from Eq. (4) and stored as separate variables for use in the algorithm.

$$\underline{C}_{BI} = \Xi^T(q)\Psi(q) \quad (4)$$

where,

$$\begin{aligned} \Xi(q) &= \begin{bmatrix} q_4 I_{3 \times 3} + [\underline{q} \times] \\ -\underline{q}^T \end{bmatrix} \\ \Psi(q) &= \begin{bmatrix} q_4 I_{3 \times 3} - [\underline{q} \times] \\ -\underline{q}^T \end{bmatrix} \end{aligned}$$

Since two measurements are used to compute the attitude quaternion the algorithm performs two iterations of Eq. (5) through Eq. (9) to calculate the sensitivity matrix H_k (Eq. (5)), Kalman gain K_k (Eq. (6)), error covariance P_k^+ (Eq. (7)), residual ϵ_k (Eq. (8)) and error state $\Delta \hat{x}_k^+$ (Eq. (9)). The parameters computed in Eq. (5) through Eq. (9) are used to update the quaternion \hat{q}_k^+ , gyro bias $\hat{\beta}_k^+$ and error covariance matrix \hat{P}_k^+ .

$$H_k = \begin{bmatrix} [\underline{C}_{BI}^T \underline{R}_i \times] & 0_{3 \times 3} \end{bmatrix} \quad (5)$$

$$K_k = P_k^- H_k^T [H_k P_k^- H_k^T + \sigma_i^2 I]^{-1} \quad (6)$$

$$P_k^+ = [I - K_k H_k] P_k^- \quad (7)$$

$$\epsilon_k = ({}^B \tilde{\underline{R}}_i - \underline{C}_{BI}^T \underline{R}_i) \quad (8)$$

$$\Delta \hat{x}_k^+ = \Delta \hat{x}_k^- + K_k [\epsilon_k - H_k \Delta \hat{x}_k^-] \quad (9)$$

$$\Delta \hat{x}_k^+ = [\delta \hat{\alpha}_k^{+T} \Delta \hat{\beta}_k^{+T}]^T \quad (10)$$

$$\hat{q}_k^+ = \hat{q}_k^- + \frac{1}{2} \Xi(\hat{q}_k^-) \delta \hat{\alpha}_k^+ \quad (11)$$

$$\hat{\beta}_k^+ = \hat{\beta}_k^- + \Delta \hat{\beta}_k^+ \quad (12)$$

The quaternion, gyro bias and the error covariance matrix computed during the attitude determination phase are passed as arguments to the attitude propagation phase. The satellite angular rates

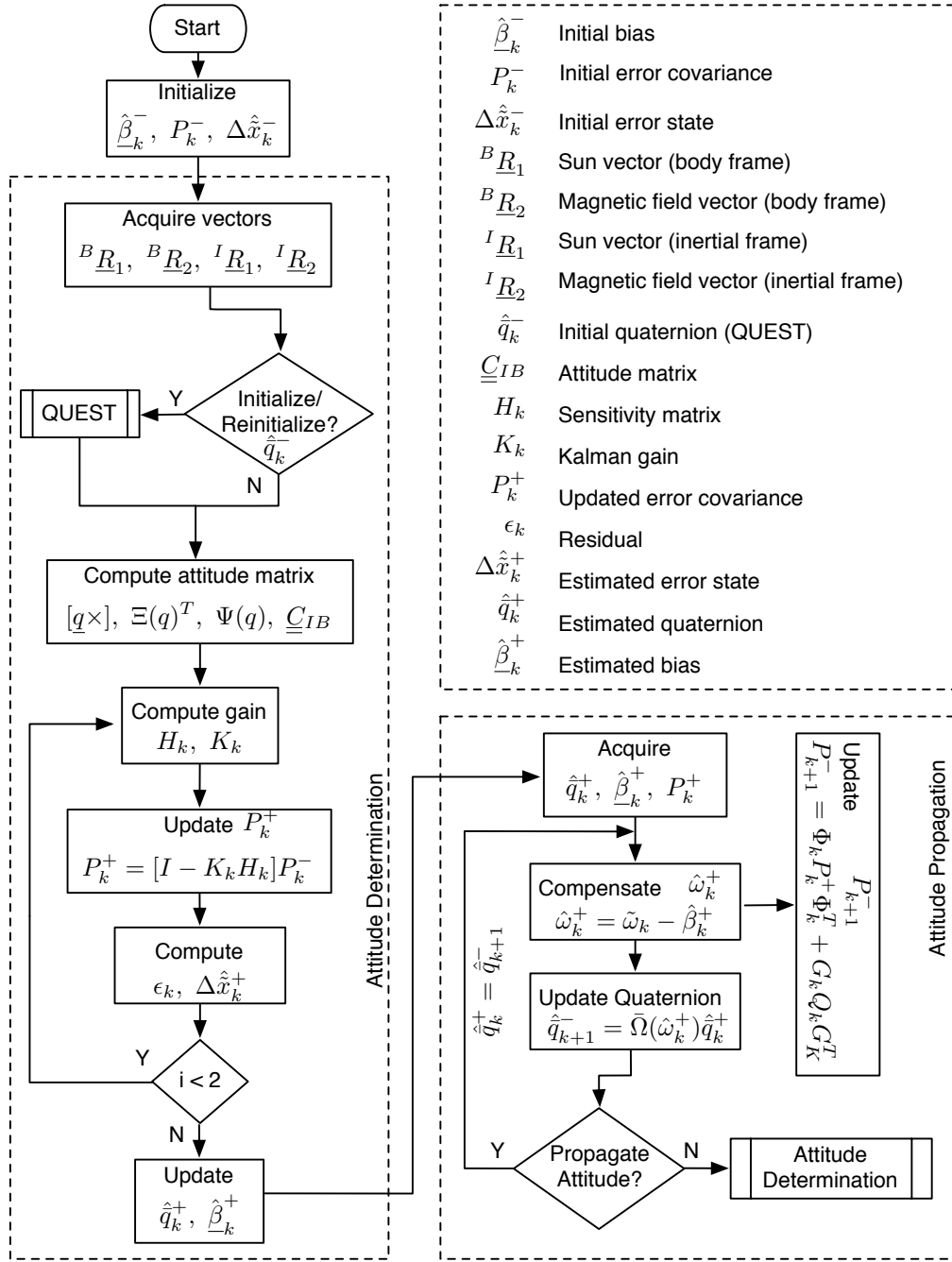


Figure 4. Attitude Estimation Algorithm for SwampSat

are acquired from the gyro measurements and the gyro bias is compensated (Eq. (13)). The estimated satellite angular rates are used within this phase to propagate the satellite attitude (Eq. (14)).

$$\hat{\omega}_k^+ = \tilde{\omega}_k - \hat{\beta}_k^+ \quad (13)$$

$$\hat{q}_{k+1}^- = \bar{\Omega}(\hat{\omega}_k^+) \hat{q}_k^+ \quad (14)$$

where,

$$\begin{aligned}\bar{\Omega}(\underline{\hat{\omega}}_k^+) &= \begin{bmatrix} \cos(\frac{1}{2}\|\underline{\hat{\omega}}_k^+\|\Delta t)I_{3\times 3} - [\hat{\psi}_k^+ \times] & \hat{\psi}_k^+ \\ -\hat{\psi}_k^{+T} & \cos(\frac{1}{2}\|\underline{\hat{\omega}}_k^+\|\Delta t) \end{bmatrix} \\ \hat{\psi}_k^+ &= \frac{\sin(\frac{1}{2}\|\underline{\hat{\omega}}_k^+\|\Delta t)\underline{\hat{\omega}}_k^+}{\|\underline{\hat{\omega}}_k^+\|}\end{aligned}$$

Additionally the error covariance matrix is also propagated using Eq. (5) through Eq. (9) during this phase to update the states of the satellite.

$$P_{k+1}^- = \Phi_k P_k^+ \Phi_k^T + G_k Q_k G_k^T \quad (15)$$

where,

$$\begin{aligned}G_k &= \begin{bmatrix} -I_{3\times 3} & 0_{3\times 3} \\ 0_{3\times 3} & I_{3\times 3} \end{bmatrix} \\ Q_k &= \begin{bmatrix} (\sigma_v^2 \Delta t + \frac{1}{3}\sigma_u^2 \Delta t^3)I_{3\times 3} & -(\frac{1}{2}\sigma_u^2 \Delta t^2)I_{3\times 3} \\ -(\frac{1}{2}\sigma_u^2 \Delta t^2)I_{3\times 3} & (\sigma_u^2 \Delta t)I_{3\times 3} \end{bmatrix} \\ \Phi &= \begin{bmatrix} \Phi_{11} & \Phi_{12} \\ \Phi_{21} & \Phi_{22} \end{bmatrix} \\ \Phi_{11} &= I_{3\times 3} - [\underline{\hat{\omega}} \times] \frac{\sin(\|\underline{\hat{\omega}}\|\Delta t)}{\|\underline{\hat{\omega}}\|} + [\underline{\hat{\omega}} \times]^2 \frac{\{1 - \cos(\|\underline{\hat{\omega}}\|\Delta t)\}}{\|\underline{\hat{\omega}}\|^2} \\ \Phi_{12} &= [\underline{\hat{\omega}} \times] \frac{\{1 - \cos(\|\underline{\hat{\omega}}\|\Delta t)\}}{\|\underline{\hat{\omega}}\|_2} - I_{3\times 3} \Delta t - [\underline{\hat{\omega}} \times] \frac{\{\|\underline{\hat{\omega}}\|\Delta t - \sin(\|\underline{\hat{\omega}}\|\Delta t)\}}{\|\underline{\hat{\omega}}\|^3} \\ \Phi_{21} &= 0_{3\times 3} \\ \Phi_{22} &= I_{3\times 3}\end{aligned}$$

Here, σ_v^2 and σ_u^2 are the variances associated with the random drift η_v and drift rate ramp η_u components of the on board gyros. The components are discussed as part of the gyro model. The sampling interval is captured by the parameter Δt . The filter is implemented in two phases to account for the distributed implementation of the attitude determination capability of SwampSat.

SIMULATION AND RESULTS

To qualify and evaluate the need and effectiveness of an attitude estimation algorithm for SwampSat, simulations are performed with data generated from satellite tool kit (STK).²² The picosatellite is assumed to be launched out of a P-POD and have angular rates of up to ± 2 deg/s about each axes. A satellite in a low earth orbit of a STK scenario initialized with these rates is considered. The satellite orbit is designed to be a low earth orbit with parameters shown in Table 1. The data generated using STK consists of the quantities shown in Table 2. The true quaternion in the data set is used for comparing the estimated quaternion from the attitude estimation algorithm. Orbital period is a function of the semimajor axis and for the LEO considered in Table 1 it is about 95 minutes. The attitude data set for each scenario is generated for 95 minutes with a 10 Hz frequency. To emulate sensor measurements on orbit the data is corrupted with bias and noise values determined from experiments, models and component data sheets. To identify the need for SwampSat attitude estimation, simulations are carried out to compare attitude determination results of a deterministic

Table 1. LEO Parameters for STK Scenario

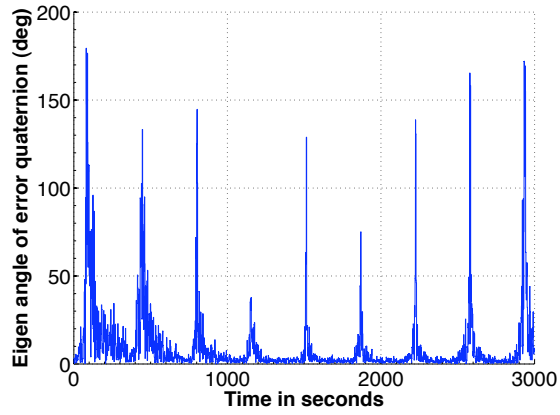
Semimajor axis (a)	6896.31 Km
Eccentricity (e)	0.07944
Inclination (i)	18.6052 deg
Argument of perigee (ω)	0 deg
Longitude of ascending node (Ω)	89.9812 deg
True anomaly (ϑ)	90.3386 deg

Table 2. Attitude Data Generated for Simulation

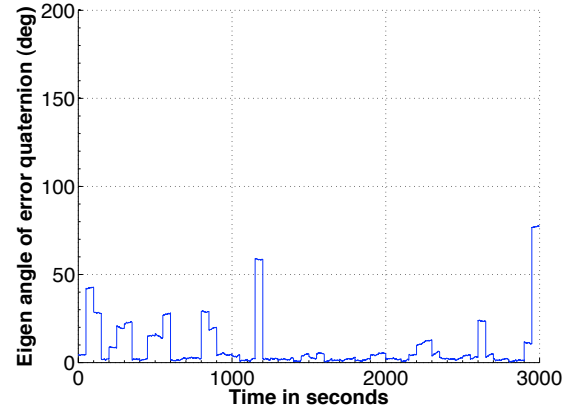
Quantity	Description
${}^B \underline{R}_1$	3x1 Sun vector coordinatized in body frame
${}^B \underline{R}_2$	3x1 magnetic field vector coordinatized in body frame
${}^I \underline{R}_1$	3x1 Sun vector coordinatized in ECI frame
${}^I \underline{R}_2$	3x1 magnetic field vector coordinatized in ECI frame
${}^B \underline{\omega}$	3x1 angular velocity vector coordinatized in body frame
\bar{q}	4x1 quaternion representing true attitude

approach with the true quaternions obtained from STK. The plots shown in Figure 5 justify the need for attitude estimation of SwampSat, particularly for rapid retargeting and precision pointing.

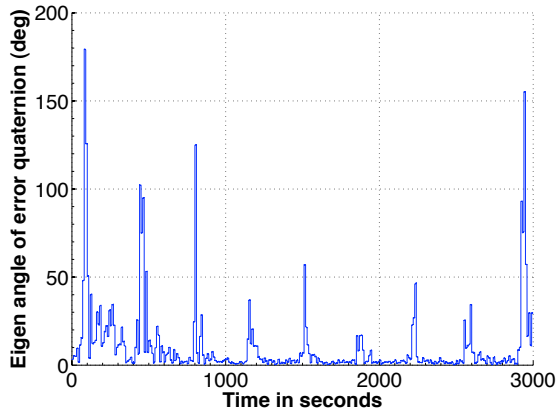
To evaluate the effectiveness of the algorithm shown in Figure 4, attitude estimation simulations are performed using the corrupted sensor measurements. The algorithm has the goal of filtering attitude vector measurements and estimate gyro biases for all three axes. A standard deviation of 5% of the magnitude of standard deviation of the vector measurements is adopted for the attitude sensors. Gyro measurements obtained by placing the ADIS16405 IMU on a stationary platform are used as noise parameters for satellite angular rate sensor. As simulation parameters the attitude error covariance is set to 4.8^2 deg^2 and the gyro drift covariance is set to 2.4 deg/sec^2 . The initial bias for each axis is assumed to be 0 deg/hr. The results of the simulation are shown in Figure 6 and Figure 7. With the available on board attitude sensors the estimation algorithm vastly improves upon the attitude determination results shown in Figure 5. It can be seen from Figure 6 that the accuracy of the attitude estimate increases with increase in the sampling frequency of the attitude sensors. The simulations are carried out for 40-50 minutes to qualify and evaluate the estimation algorithm for SwampSat maneuvers. The estimation algorithm has the capability to provide better accuracies of relative attitude than the absolute values. The estimation algorithm requires a finite time to converge to a steady error but this is accommodated in the SwampSat system.



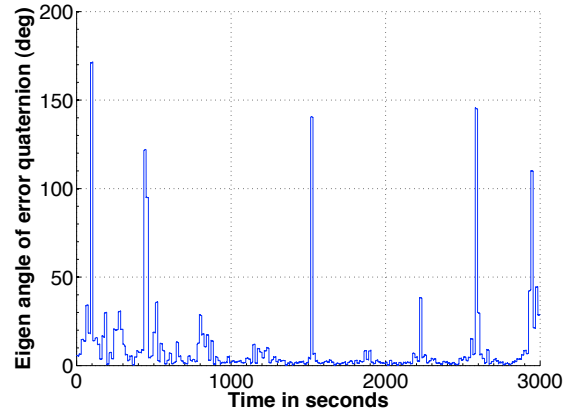
(a) Attitude Sensors Sampled Every 2 Seconds



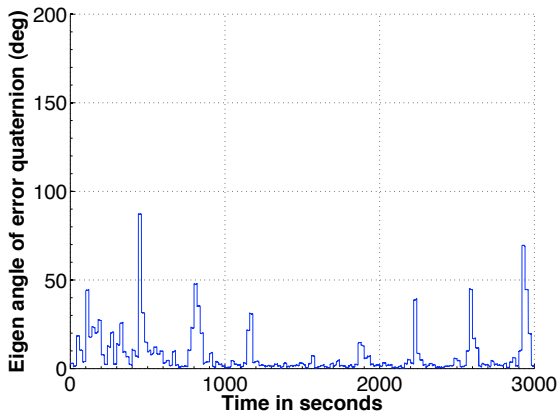
(b) Attitude Sensors Sampled Every 5 Seconds



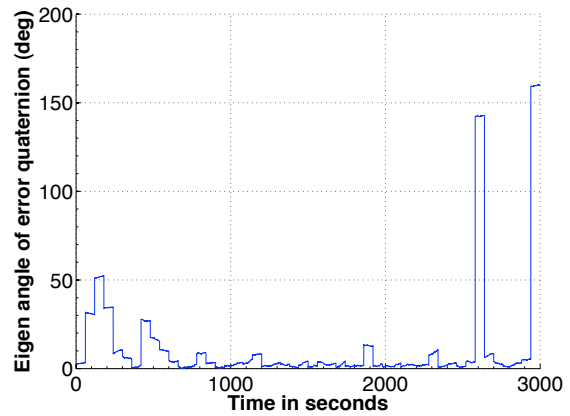
(c) Attitude Sensors Sampled Every 10 Seconds



(d) Attitude Sensors Sampled Every 15 Seconds

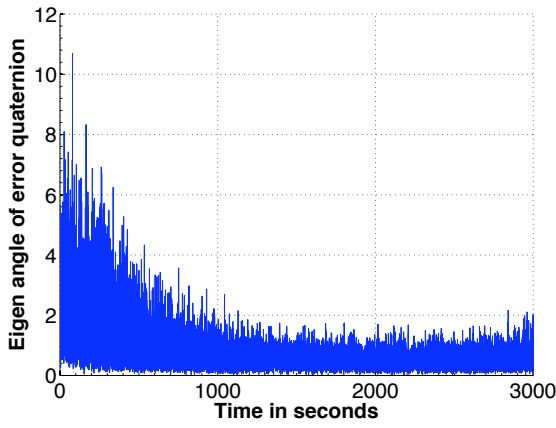


(e) Attitude Sensors Sampled Every 20 Seconds

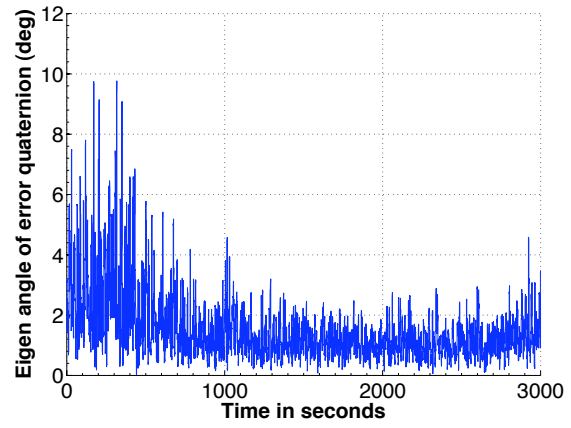


(f) Attitude Sensors Sampled Every 1 Minute

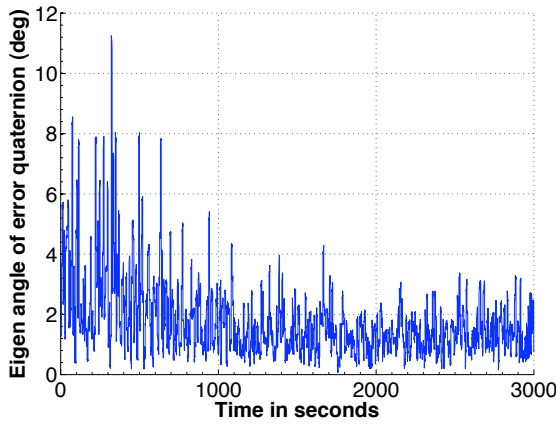
Figure 5. Plot of ADS Error - Eigen Angle of Error Quaternion



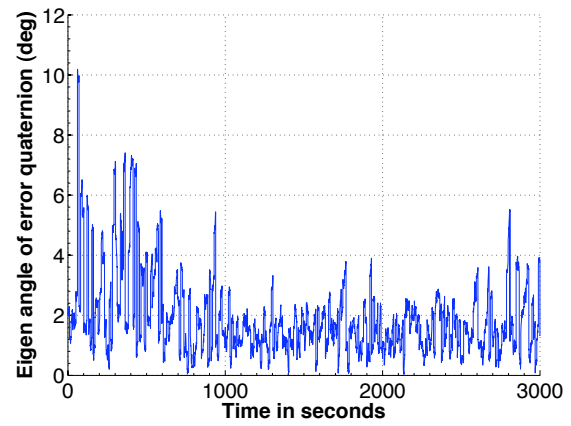
(a) Attitude Sensors and Gyros Sampled Alternatively



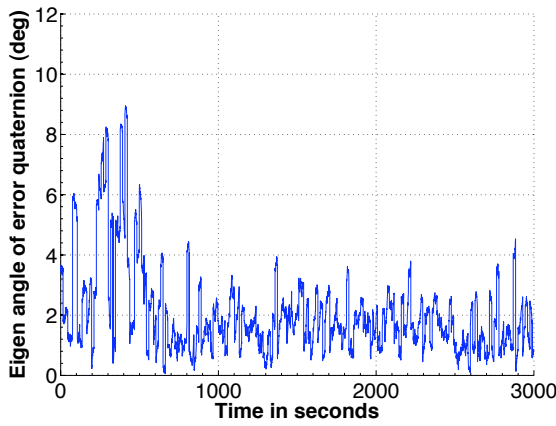
(b) Attitude Sensors Sampled Every 2 Seconds



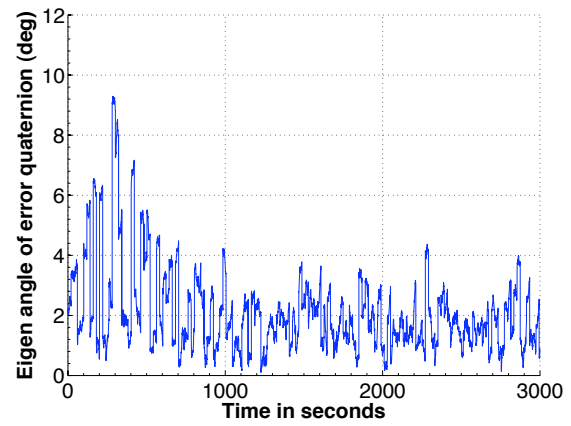
(c) Attitude Sensors Sampled Every 5 Seconds



(d) Attitude Sensors Sampled Every 10 Seconds

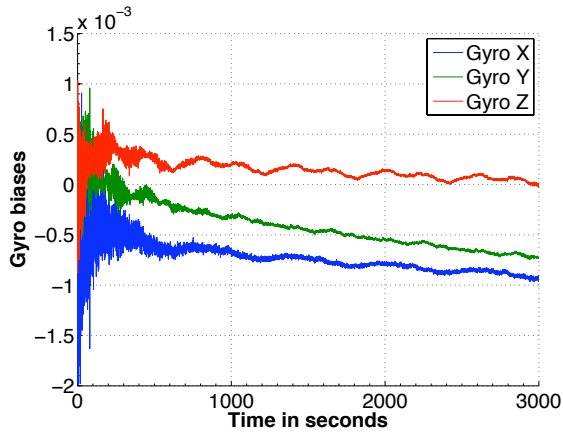


(e) Attitude Sensors Sampled Every 15 Seconds

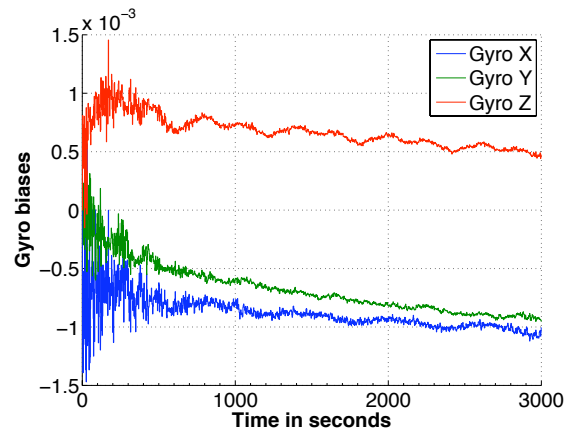


(f) Attitude Sensors Sampled Every 20 Seconds

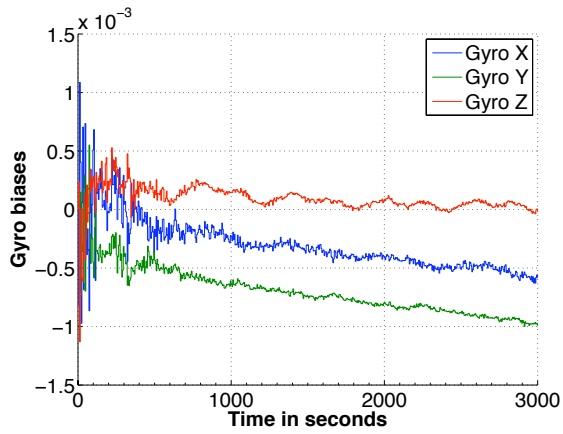
Figure 6. Plot of Estimation Error - Eigen Angle of Error Quaternion



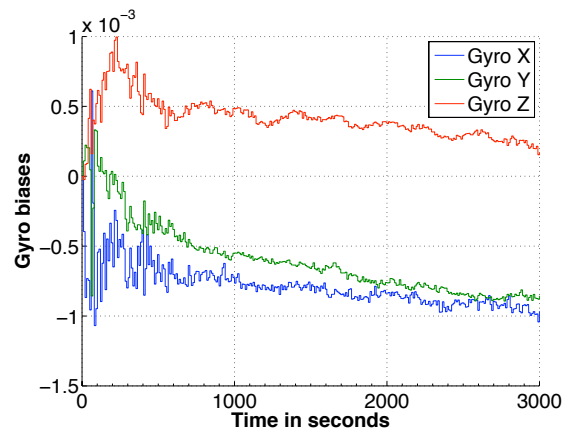
(a) Attitude Sensors and Gyros Sampled Alternately



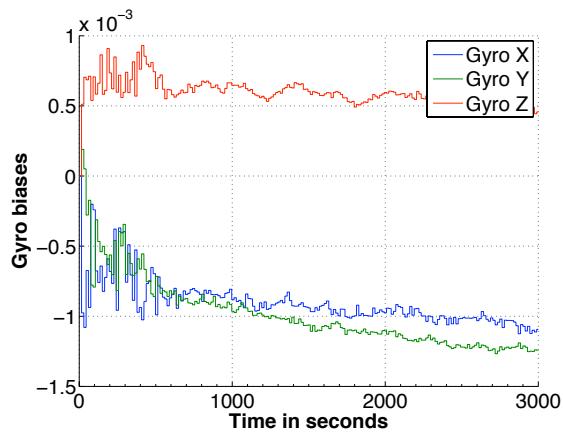
(b) Attitude Sensors Sampled Every 2 Seconds



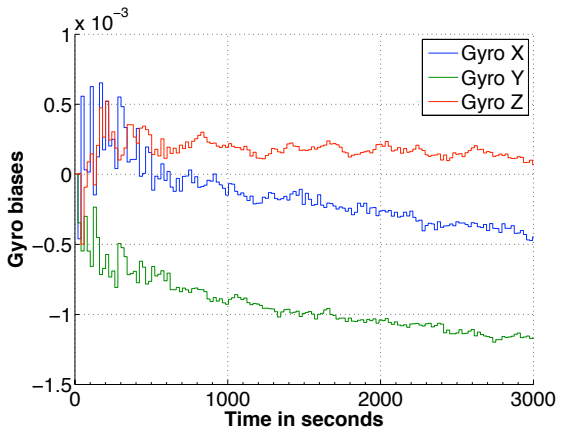
(c) Attitude Sensors Sampled Every 5 Seconds



(d) Attitude Sensors Sampled Every 10 Seconds



(e) Attitude Sensors Sampled Every 15 Seconds



(f) Attitude Sensors Sampled Every 20 Seconds

Figure 7. Plot of Estimated Gyro Bias

CONCLUSION

An algorithm adapted for estimating the attitude of a picosatellite with a distributed computing platform is discussed. The distributed platform addresses the computational limitation and an approach for utilizing the on board power resources effectively. The adaptation presents a design for implementing an attitude determination and estimation system for nano- and picosatellites of the CubeSat form factor. Murrell's EKF is selected over conventional EKF to improve on the computational efficiency^{6,10} and QUEST is used as an initial attitude estimate for faster convergence with the true attitude. The operations' design shown in Figure ?? summarize the approach for executing the estimation algorithm for ADS and ACS validation on orbit. The simulation results shown in Figure 5 and Figure 6 justify the need and effectiveness of attitude estimation for a picosatellite hosting the type of sensors discussed above.

The distributed platform in an effort to overcome the SWaP limitation of a CubeSat, introduces uncertainties in the form of time delays between the two computing units. The paper makes a case for investigating the effect of time delays on the attitude estimate and control authority. The efficiency of Murrell's EKF over conventional EKF needs to be quantified for the distributed platform of SwampSat. The paper makes a case for an implementation supporting the parallel operation of attitude determination and control algorithms. The advantages and limitations of such an implementation need to be investigated.

ACKNOWLEDGMENT

The authors wish to acknowledge the support of SwampSat development team, specifically Shawn Allgeier, Dante Buckley, Katie Cason, Takashi Hiramatsu, Shawn Johnson, Tzu Yu Lin, Matthew Mahin, Josue Munoz, Vivek Nagabhushan, Kunal Patankar, Bungo Shiotani, and Sal Torre.

REFERENCES

- [1] F. Leve, S. Allgeier, V. Nagabhushan, S. Asundi, D. Buckley, A. Waldrum, and T. Hiramatsu, "ASTREC-I Detailed Design Report, FUNSAT IV Design Competition," 2007-2008.
- [2] "Office of the Chief Technologist: Small Spacecraft Program," http://www.nasa.gov/pdf/474015main.SmallSat_Conference.8_9_10.pdf, 2010.
- [3] F. Leve, "Development of the Spacecraft Orientation Buoyancy Experimental Kiosk," Master's thesis, University of Florida, 2008.
- [4] V. Nagabhushan, "Development of control moment gyroscopes for attitude control of small satellites," Master's thesis, University of Florida, 2009.
- [5] M. Shuster and S. Oh, "Three-axis attitude determination from vector observations," *Journal of Guidance and Control*, Vol. 4, No. 1, 1981, pp. 70-77.
- [6] J. Murrell, "Precision attitude determination for multitemission spacecraft," *Guidance and Control Conference, Palo Alto, Calif., August 7-9, 1978, Technical Papers.(A78-50159 22-01)* New York, American Institute of Aeronautics and Astronautics, Inc., 1978, p. 70-87., 1978.
- [7] R. Kalman, "A new approach to linear filtering and prediction problems," *Journal of Basic Engineering*, Vol. 82, No. 1, 1960, pp. 35-45.
- [8] R. Kalman and R. Bucy, "New results in linear filtering and prediction theory," *Random Processes*, 1973.
- [9] M. Shuster, E. Lefferts, and F. Markley, "Kalman Filtering for Spacecraft Attitude Estimation," *AIAA 20th Aerospace Sciences Meeting, Orlando, Florida*, Vol. 232, 1982.
- [10] J. Crassidis and J. Junkins, *Optimal estimation of dynamic systems*. Chapman & Hall, 2004.
- [11] R. Munkata, "CubeSat Design Specification Rev. 12," August, 2009.
- [12] J. Puig-Suari, C. Turner, and W. Ahlgren, "Development of the standard CubeSat deployer and a CubeSat class PicoSatellite," *Aerospace Conference, 2001, IEEE Proceedings.*, Vol. 1, 2001.

- [13] I. Garcia, "Texas Instruments Application Report - TMS320C6711D, C6712D, C6713B Power Consumption Summary," <http://focus.ti.com/lit/an/spra889a/spra889a.pdf>, 2005.
- [14] "MSP430 16-bit Ultra-Low Power Micorcontroller," www.ti.com/msp430.
- [15] "C6000 High Performance DSP," <http://focus.ti.com/paramsearch/docs/parametricsearch.tsp?family=dspsectionId=2tabId=57familyId=132>.
- [16] S. Allgeier, M. Mahin, and N. Fitz-Coy, "Design and Analysis of a Coarse Sun Sensor for Pico-Satellites," *Proceedings of the AIAA Infotech@ Aerospace Conference*, 2009.
- [17] "Honeywell Magnetometer HMC2003," <http://www.ssec.honeywell.com/magnetic/datasheets/hmc2003.pdf>.
- [18] J. Crassidis and F. Markley, "Unscented filtering for spacecraft attitude estimation," *Journal of Guidance Control and Dynamics*, Vol. 26, No. 4, 2003, pp. 536–542.
- [19] "Analog Devices Tri-Axis Inertial Sensor with Magnetometer ADIS16405," http://www.analog.com/static/imported-files/data_sheets/ADIS16405.pdf.
- [20] R. Farrenkopf, "Analytic Steady-State Accuracy Solutions for Two Common Spacecraft Attitude Estimators," *Journal of Guidance and Control*, Vol. 1, No. 4, 1978, pp. 282–284.
- [21] D. Hoffman and T. McElroy, "HEAO attitude reference design," *American Astronautical Society, Annual Rocky Mountain Guidance and Control Conference, Keystone, Colo., Mar. 10-13, 1978, 21 p.*, 1978.
- [22] "Analytical Graphics, Inc. (AGI) - Satellite Tool Kit (STK)," <http://www.stk.com/>.